ChemSearch Journal 15(2): 54 – 66, December, 2024
Publication of Chemical Society of Nigeria, Kano Chapter

Received: 10/08/2024 Accepted: 07/11/2024
http://www.ajol.info/index.php/csj

Efficient Dye Removal using Cellulose-TiO_2 Nanocomposites Synthesized from Millet Husk

Magaji Ladan[1*], Ali Salisu[2], and Shehu Habibu[1]
[1]Department of Pure and Industrial Chemistry, Faculty of Physical Sciences, Bayero University Kano, P.M.B. 3011 BUK, Kano – Nigeria
[2]Department of Chemistry, Faculty of Natural & Applied Sciences, Sule Lamido University Kafin Hausa, P.M.B. 048, Jigawa State – Nigeria
***Correspondence Email:** mladan.chm@buk.edu.ng

ABSTRACT
Cellulose was successfully isolated from millet husk via the Alkaline-Hydrogen peroxide method and Cel/TiO_2 NCs were synthesized via the sol-gel process. The extracted cellulose was used to increase the adsorption efficiency of TiO_2. The adsorbents were characterized using FTIR, SEM, and XRD analysis. FTIR spectra of the nanocomposites show that the TiO_2 is bound to the hydroxyl group of the cellulose by hydrogen bonding. A batch adsorption study was carried out to test the effectiveness of the adsorbents on the adsorption of methylene blue (MB) and methyl orange (MO), optimum conditions for the adsorption were found to be 0.5g/100mL at an initial dye concentration of 18mg/L, 25^{o}C, 20 minutes and pH of 8 for MB while 25 minutes and pH 4 for MO. The crystallite size of Cel/TiO_2 NCs was calculated using the Scherrer equation to be 27.6nm. MB was effectively desorbed using 0.1 mol/L NaOH solution from the adsorbents and the adsorbent exhibited a good reusability. The adsorption data fit the pseudo-second-order model for adsorption kinetics and the Langmuir model for adsorption isotherms. Thermodynamic analysis revealed that the adsorption process was chemisorption, spontaneous, feasible, and endothermic. These findings suggest that the adsorbents could be an economical and efficient solution for removing dyes from wastewater.

Keywords: Adsorbent, Adsorption, Cellulose, Millet husk, Nanocomposites

INTRODUCTION

The rapid industrialization and urbanization have led to a significant increase in water pollution, particularly from dye-containing effluents released by textile, leather, and paper industries. These dyes, being chemically stable and often toxic, pose a serious threat to aquatic life and human health (Dutta *et al.*, 2024; Mehra *et al.*, 2021; Srivastava & Sofi, 2020). Conventional wastewater treatment methods, such as chemical coagulation, oxidation, and biological degradation, often fall short in effectively removing dyes due to their complex molecular structures and resistance to biodegradation (Giwa *et al.*, 2021; Habibu *et al.*, 2023; Katheresan *et al.*, 2018).

In recent years, nanotechnology has emerged as a promising approach for environmental remediation, offering high surface area, reactivity, and adsorption capacities (Guerra *et al.*, 2018; Khan *et al.*, 2021; Khin *et al.*, 2012). Among various nanomaterials, titanium dioxide (TiO_2) nanoparticles have garnered significant attention due to their excellent photocatalytic properties, chemical stability, and low toxicity (Ghosh & Das, 2015; Ma *et al.*, 2014; Mahlambi *et al.*, 2015). However, the aggregation of TiO_2 nanoparticles and their recovery from treated water remain challenging issues.

To address these challenges, the development of nanocomposites by integrating TiO_2 with biocompatible and biodegradable materials such as cellulose has shown great potential. Cellulose, being the most abundant natural polymer, offers numerous advantages including high mechanical strength, renewability, and environmental friendliness (Khalil *et al.*, 2012; Li *et al.*, 2021; Shaghaleh *et al.*, 2018). Utilizing agricultural waste, such as millet husk, as a source of cellulose not only adds value to these by-products but also promotes sustainability.

The present study focuses on the synthesis of cellulose-TiO_2 nanocomposites from millet husk and the evaluation of their efficiency in dye removal from wastewater. By leveraging the synergistic properties of cellulose and TiO_2, the research aims to develop an economical and effective adsorbent material. This novel approach not only provides a solution to wastewater treatment but also contributes to waste valorization, aligning with the principles of green chemistry and sustainable development.

MATERIALS AND METHODS

All chemicals used in this research were of analytical grade and used without further purification. These include methanol, ethanol, sodium hydroxide, titanium tetra-isopropoxide (TTIP), 95.6% glacial acetic acid, hydrogen peroxide, benzene, millet husk, methylene blue, and methyl orange.

Sample Collection and Pre-treatment

The millet husk sample was obtained from Tamasu Gari farmhouse, Kwalam town, Taura Local Government area of Jigawa state, Nigeria. The husk was washed under tap water to remove adhering materials, dried at room temperature, ground into fine particles and sieved using 30 mesh size.

Isolation of Cellulose from Millet Husk

The dried waste was extracted with (2:1 v/v) benzene-methanol for 6 hrs in a soxhlet apparatus to remove lignin, and dried in an oven at 50ºC for 17hrs. The dewaxed sample was soaked in alkaline-hydrogen peroxide solution prepared by mixing 1% alkaline sodium hydroxide solution (1%; NaOH/H_2O; 1g/100ml) and 20% hydrogen peroxide solution (20%; H_2O_2/H_2O; 33.36mL/166.7mL) at 100 ºC for 1hr 30 min to remove hemicellulose, filtered and washed several times with distilled water until neutral pH and then dried in an oven at 60ºC for 5hrs (Sheltami *et al*., 2012).

Synthesis of Cel/TiO_2 NCs

Cel/TiO_2NCs were prepared using titanium tetra-isopropoxide (TTIP) and the cellulose extract from millet husk as a precursor via the sol-gel method. The method used was earlier described in the literature (Ladan *et al*., 2021). TTIP and cellulose were dissolved in 95.6% glacial acetic acid, distilled deionized water was added to the solution to complete the polycondensation (molar ratio 1:10:200 TTIP: acetic acid: DDI H_2O), the mixture was constantly stirred for 6hrs at room temperature, the resultant gel was dried at 80ºC for 5hrs.

Preparation of Stock Solution

The stock solutions of 1000 mg/L dyes were prepared by weighing 0.25g of each of Methylene Blue (MB) and Methyl orange (MO). The weighed dyes were transferred into two separate 250 cm^3 volumetric flasks and then made up to the mark with distilled water. The standard solutions used for all the experiments were prepared from the stock solutions using dilution formula.

Characterization Techniques

The morphology of the prepared Cellulose-TiO_2 nanocomposites were studied by field-emission scanning electron microscopy (FESEM) (Hitachi, model: SU8220). The chemical structure of the prepared Cellulose-TiO_2 nanocomposites was characterized by Fourier transformed infrared (FT-IR) spectrophotometer (spectrum 400) over a wavelength range of 400−4000 cm^{-1}. The X-Ray diffraction (XRD) was performed using Siemens D5000, with a Cu-Kα radiation source mounted on a horizontal θ-2θ goniometer.

Adsorption Study

Batch adsorption experiments were conducted to study the adsorptive behavior of cellulose extract and Cel/TiO_2 NCs for adsorption of cationic (MB) and anionic (MO) dyes. 0.5g of cellulose extract was added to 100 mL of 18mg/L MB solution, the solution was magnetically stirred at room temperature, 4 mL of the MB solution was taken out at a predetermined time and analyzed using UV spectrophotometer after proper centrifugation. To study the adsorption kinetics, the reaction was presumed to be completed when the dye solution became colorless and at this stage the measurements were stopped. Batch adsorption experiments for MO were also conducted using the same adsorbent. Furthermore, for comparison the adsorption studies of Cel/TiO_2 NCs were carried out on MB and MO using the same procedure. The adsorptive capacity Q_t (mg/g) and dye removal efficiency were calculated using equations 1 and 2.

$$Q_t = \frac{C_\circ - C_t}{m} \quad (1)$$

$$Removal\ efficiency\ (\%) = \frac{C_\circ - C_e}{C_e} \text{ x } 100 \quad (2)$$

where C_o (mg/L) is the initial concentration of the dye solution, C_t (mg/L) is the concentration of the dye solution at time t, C_e (mg/L) is the dye concentration at equilibrium, V (L) is the initial volume of the dye solution and m (g) is the adsorbent mass (Li *et al*., 2019).

Kinetic Studies

The kinetics of adsorption of MB and MO adsorption onto cellulose and Cel/TiO_2 NCs were determined using the data of effect of contact time. Pseudo-first order and Pseudo-second order models were used to predict the adsorption behavior and rate of the adsorbate uptake onto the adsorbent.
Pseudo-first order model is represented as:

$$\ln = \frac{[C]_\circ}{[C]_t} = \ln \frac{(A)_\circ}{(A_t)} = k_t \quad (3)$$

Where: k represents the rate constant (min^{-1}), C_o and C_t are the initial and final concentration of the dye solution, A_o and A_t are the initial and final absorbance of the dye solution, k is the slope of the plot of ln $[C]_o/[C]_t$ against time (t) as shown in Figures 9 and 10 (Rashid *et al.*, 2022)

Pseudo-second order model based on adsorption equilibrium capacity is given in equation 4:

$$\frac{t}{Q_t} = \frac{1}{k_2 Q_e^2} + \frac{1}{Q_e} t \quad (4)$$

Where: k_2 (g/mg/min) is the rate constant for pseudo-second order adsorption process, Q_e and k_2 are calculated from the slope and intercept of the linear plot of t/Q_t versus time (t) as shown in Figures 9 and 10 (Tang *et al.*, 2017).

Thermodynamic Studies

The adsorption of MB and MO onto Cellulose and Cel/TiO_2 NCs were studied by analyzing the effect of temperature. Equations 5, 6, 7 and 8 were used to determine the feasibility and spontaneity of the adsorption process. Additionally, a plot of $\ln K_c$ against 1/T was used to obtain the enthalpy (ΔH), Entropy (ΔS) and Gibb's free energy (ΔG) for the adsorption process.

$$\Delta G = \Delta H - T\Delta S \quad (5)$$

$$\Delta G = -RT\ln K \quad (6)$$

$$\ln K = \frac{\Delta S}{R} = -\frac{\Delta H T}{R} \quad (7)$$

$$K = \frac{C_\circ - C_e}{C_e} \quad (8)$$

Where R is the molar gas constant, T is the absolute temperature in kelvin (K), ΔH(kJmol^{-1}) is the enthalpy change, ΔS (JmolK^{-1}) is the entropy changes. ΔG (kJ/mol) is the Gibbs free energy changes and K is the ratio of the dye concentration on adsorbent at equilibrium (Q_e) to the remaining dye concentration in solution at equilibrium (C_e). The slope and intercept of the linear plot of lnK versus 1/T were used to determine the value of ΔHand ΔS respectively (Rashid *et al*., 2022).

Isotherm Studies

Adsorption isotherm is used to determine how the adsorbate molecules are distributed between the liquid phase and adsorbent. Equilibrium adsorption data were used to determine the adsorption isotherm, where both Langmuir and Freundlich isotherm models were applied.

Langmuir Isotherm Model

This model is based on the assumption that monolayer adsorption occurs on a homogeneous surface and all the adsorption sites on the adsorbate material are homogeneous, it can be written as equation 9.

$$\frac{C_e}{Q_e} = \frac{1}{Q_m K_L} + \frac{C_e}{Q_m} \quad (9)$$

Where: Q_e (mg/g) is the equilibrium adsorption capacity, C_e (mg/L) is the equilibrium concentration of the dyes, K_L (l/mg) is the Langmuir isotherm constant, Q_m (mg/g) is the maximum monolayer coverage adsorption capacity, the slope and intercept of the linear plot of C_e/Q_e against C_e is the value of $1/Q_m$ and $1/K_L Q_m$ respectively (Anbia and Salehi, 2012).

Dimensionless Separation Factor (R_L)

This is the essential characteristic of Langmuir model, reflecting the favorability of an adsorption process which is express as equation 10.

$$R_L = \frac{1}{1 + K_L C_m} \quad (10)$$

Where K_L is Langmuir constant, C_m (mg/L) is the maximum initial concentration of the adsorbates solution. The value of R_L indicates whether the adsorption is linear ($R_L = 1$), irreversible ($R_L = 0$), favourable equilibrium ($0 > R_L > 1$) or unfavorable equilibrium ($R_L < 1$) (Yang *et al.*, 2020).

Freundlich Isotherm Model

This model assumes that multilayer adsorption of adsorbate occurs at the heterogeneous surface of the adsorbent and all adsorption sites are heterogeneous. This model is written as equation 11.

$$\ln Q_e = \ln K_F + \frac{1}{n} \ln C_e \quad (11)$$

Where: C_e (mg/L) is the equilibrium concentration of the dyes, Q_e(mg/g) is the adsorption capacity at equilibrium K_F ((mg/g) (l/mg)$^{1/n}$) is the Freundlich isotherm constant and 1/n is the Freundlich adsorption intensity parameter. The slope and intercept of the linear plot of $\ln Q_e$ against $\ln C_e$ provided the value of 1/n and $\ln K_F$ for equation 11.

Reusability study

The used adsorbent (MB onto Cellulose and Cel/TiO_2NCs) was treated with 0.1M NaOH and distilled water as desorbing agent for 24hrs at room temperature. The resulting adsorbent was washed with deionized water to neutral pH and dried (Ahmad & Ansari, 2021). The adsorption and desorption experiments were repeated five times and the % desorption was calculated using equation 12.

$$\% \text{ desorption} = \frac{concentration\ desorbed\ (\frac{mg}{L})}{concentration\ adsorbed\ (\frac{mg}{L})} x\ 100 \quad (12)$$

RESULTS AND DISCUSSION

FTIR

The overlay FTIR spectra of Cellulose and that of Cel/TiO_2 NCs were shown in Figure 1a, with a prominent peak at around 3300, 2800, strong peak at around 1030 and a sharp peak at around 890 cm^{-1} were assigned to hydroxyl stretching vibration, C-H single bond stretching, C-O stretching vibration of primary alcohol and beta glycosodic linkage between two cellulose monomers stretching respectively. The decrease in

the intensity of hydroxyl and C-O peak of primary alcohol in the FTIR spectra of Cel/TiO_2 NCs is an indication that TiO_2 has been successfully loaded onto cellulose and the TiO_2 bound to the cellulose through hydroxyl group by hydrogen bonding. The overlay FTIR spectra of the adsorbent after adsorption of the dyes were shown in Figures 1b – 1c, decrease in the intensity of some peaks were observed which is an indication that the adsorption has taking place.

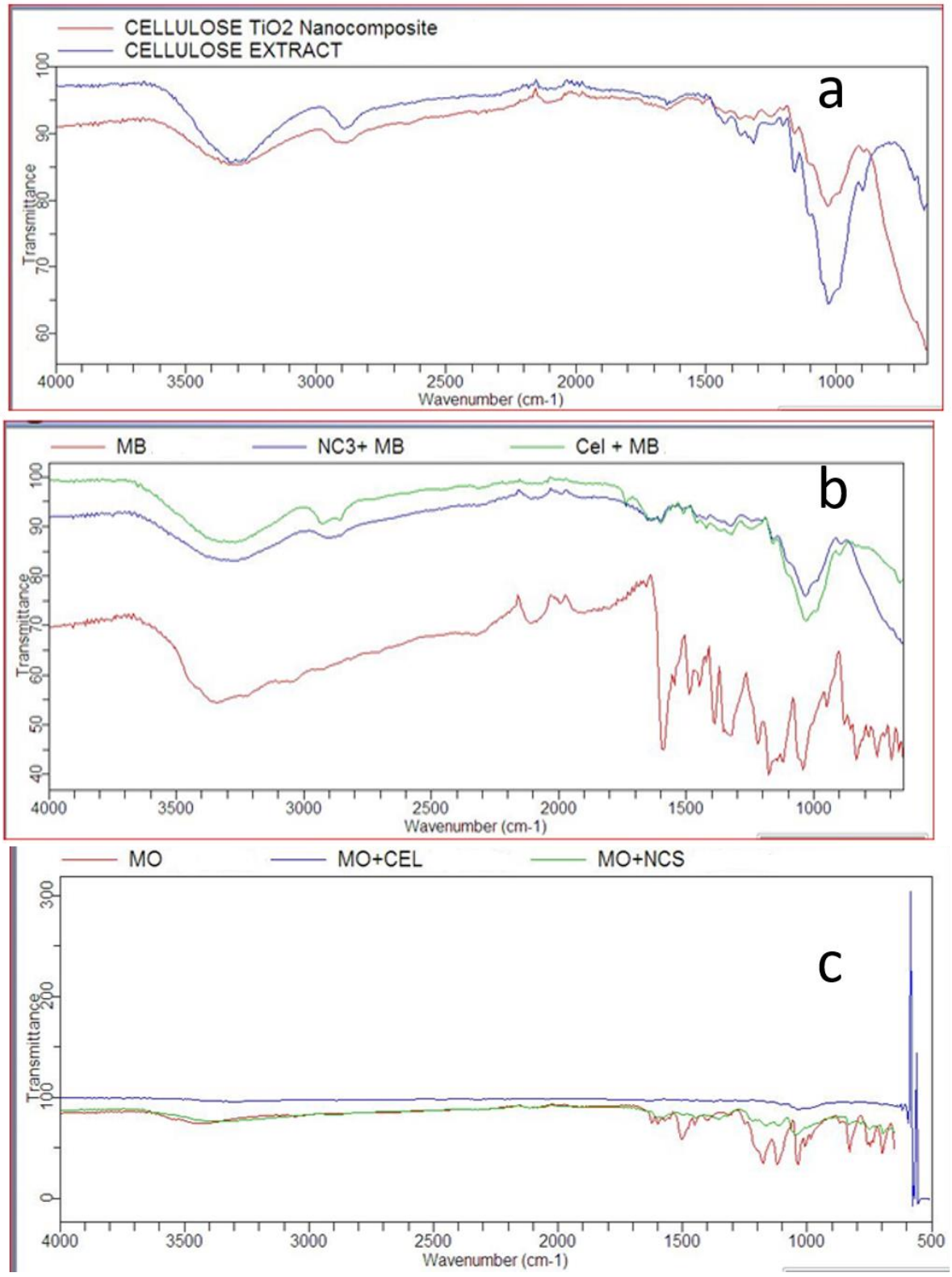

Figure 1: FTIR Spectra of (a) Cellulose and Cel/TiO_2NCs (b) MB and adsorbents after adsorption of MB(c) MO and adsorbents after adsorption of MO

X-ray Diffraction (XRD)

The crystalline characteristics of the synthesized Cel/TiO_2 NCs and that of TiO_2 NPs were investigated using XRD analysis, as shown in Figures 2a and 2b. Important peaks of anatase TiO_2 along with that of cellulose were observed in the XRD spectra of Cel/TiO_2 NCs which confirm that TiO_2 was successfully loaded onto cellulose.

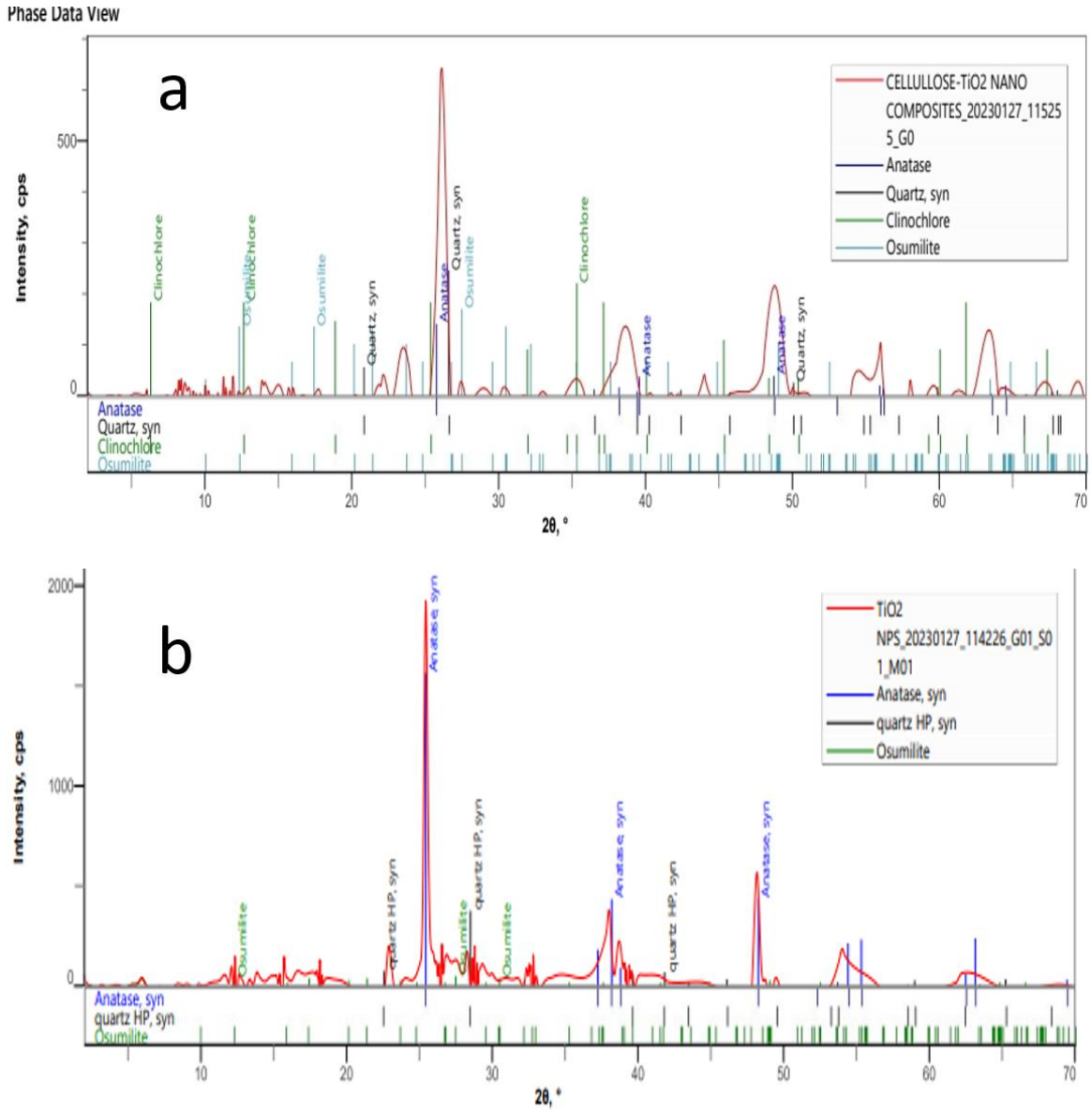

Figure 2. XRD Spectra of (a) Cel/TiO_2 NCs and (b) TiO_2 NPs

Scanning Electron Microscopy (SEM) Result

Figures 3a and 3c show the SEM micrographs of the cellulose extract and Cel/TiO_2 NCs which reveal rough, irregular shapes with a high degree of porosity, the filled pores in the SEM images of the adsorbents after adsorption is an indication that adsorption has taken place as shown in Figures 3b and 3d.

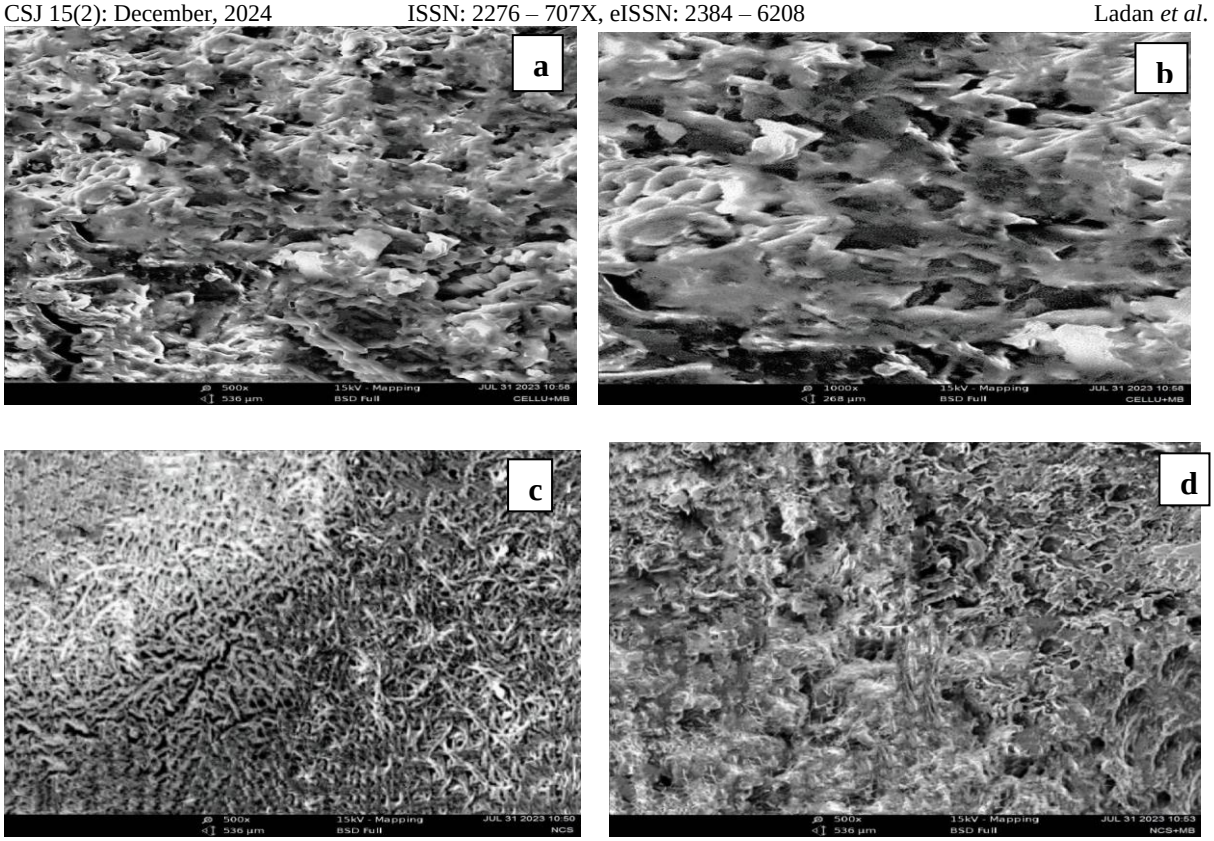

Figure 3: SEM Micrograph of Cellulose extract (a) before and (b) after adsorption of MB. Of Cel/TiO_2 NCs (c) before and (d) after adsorption of MB

Effect of Temperature

Temperature effects on the on adsorption of MB and MO onto Cellulose and Cel/TiO_2 NCs were studied at 25°C, 30°C, 35°C, 40°C, 45°C and 50°C. The results are presented in Figure 4. It was observed that increase in temperature increased the adsorbate removal efficiency up to 40°C with maximum adsorption at 45°C. This is due to an increase in mobility of the dye molecules and an increase in the number of adsorption sites. The increase in adsorption capacity due to increase in temperature accounts for the endothermic nature of the adsorption process. However, the adsorption capacity decreased when the temperature reached 50°C. This is attributable to the weakening of the adsorptive force between the active site of the adsorbent and the adsorbate, resulting in the reduction of the adsorption capacity (Rashid *et al*., 2022). Hence, it can be concluded that the optimum temperature for the adsorption of both cationic and anionic dyes onto the cellulose and Cel/TiO_2 NCs is 45°C.

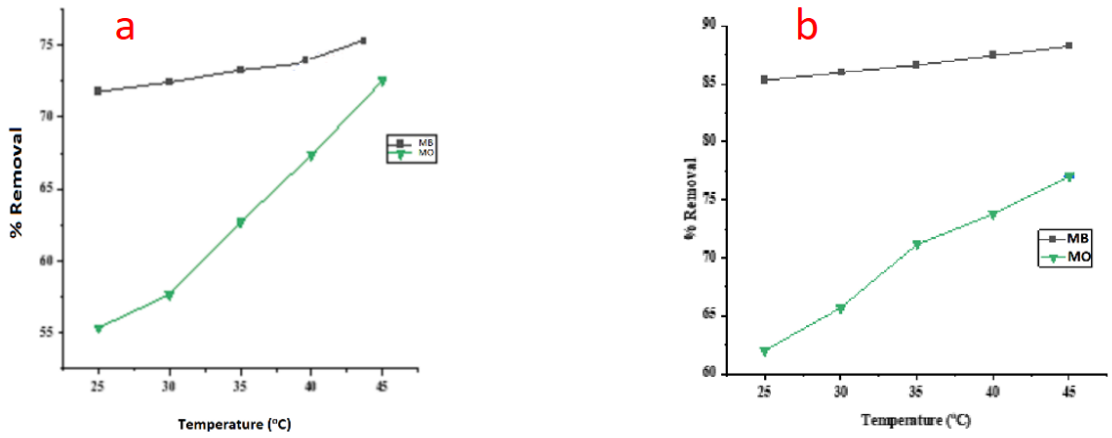

Figure 4: Effect of Temperature (°C) on MB and MO adsorption onto (a) Cellulose and (b) Cel/TiO_2 NCs

Effect of contact time

The effect of contact time on the adsorption of MB and MO onto Cellulose and Cel/TiO_2 NCs over the range of time (0-30 minutes) from aqueous solution was studied and the results are presented in Figures 5. It was observed that the maximum adsorption occurred within 20 minutes for the cationic dye (MB) and within 25 minutes for the anionic dye (MO). Furthermore, the rate of adsorbate uptake was very high in the beginning which is due to the availability of active sites on the adsorbent and high concentration gradient, which later leveled up and reached equilibrium at 20 and 25 minutes for cationic and anionic dyes respectively for adsorption onto Cel/TiO_2 NCs and Cellulose.

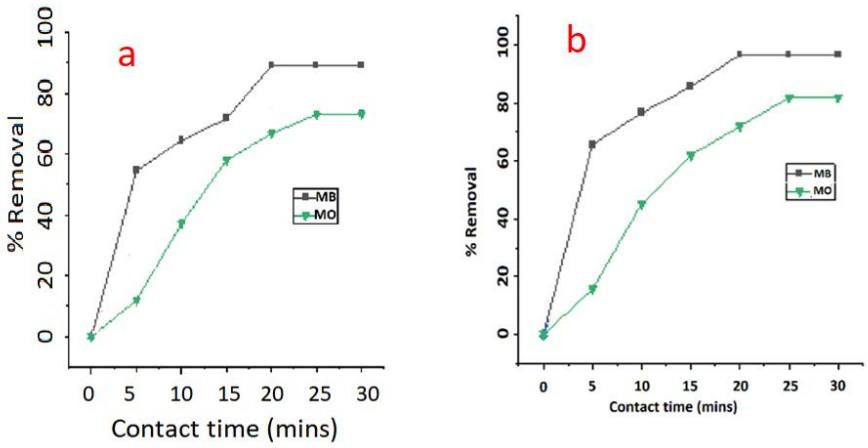

Figure 5: Effect of contact time on adsorption of MB and MO onto (a) Cellulose and (b) Cel/TiO_2 NCs

Effect of Initial Concentration

The influence of initial dye concentration on adsorption of MB and MO onto Cellulose and Cel/TiO_2 NCs from aqueous solution was studied by increasing the initial concentration (0 – 18mg/L) keeping other parameters constant as mention earlier, the results were shown in figures 6, it was observed that increase in initial concentration of the adsorbate decreases the adsorption capacity, this is because as the dye concentration rises, the remaining unoccupied adsorption sites becomes limited this can lead to saturation of the adsorption site on the surface, reducing the capacity for additional molecules to adhere.

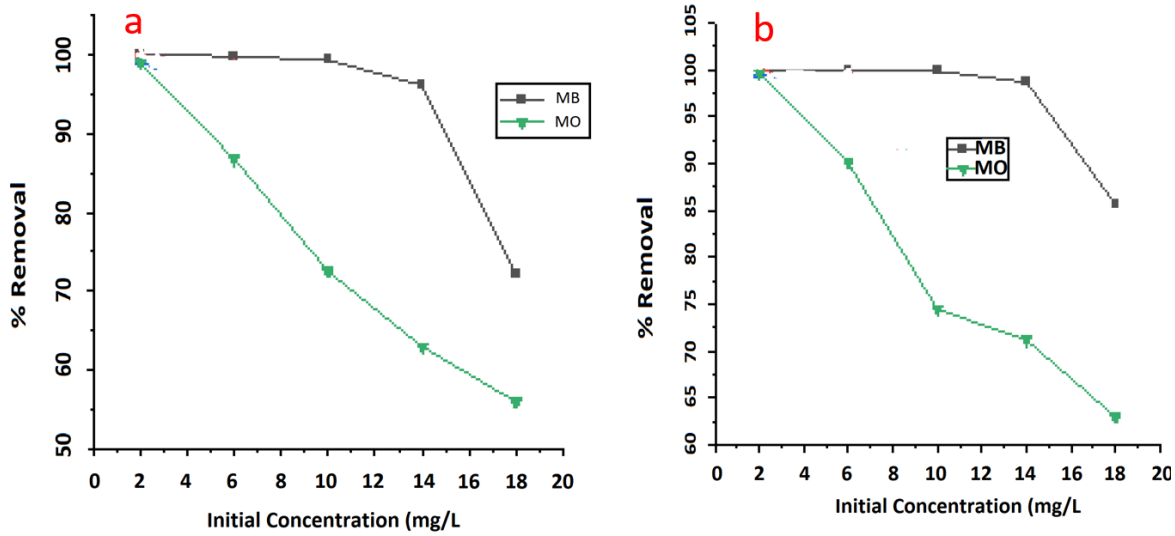

Figure 6: Effect of initial concentration on MB, and MO adsorption onto (a) Cellulose and (b) Cel/TiO_2 NCs

Effect of adsorbent Dosage

The effect of adsorbent dosage on adsorption of MB and MO onto Cellulose and Cel/TiO_2 NCs from aqueous solution was studied by increasing the adsorbent dosage from 0.1g to 0.6g keeping other parameters constant as mentioned earlier, the results are shown in Figure 7. It was observed that increase in adsorbent dosage increased the adsorption capacity for both cationic and anionic dyes this is due to an increase in the number of adsorption sites, optimum adsorption efficiency was reached when 0.5g of the adsorbents were used (Rashid *et al.*, 2022).

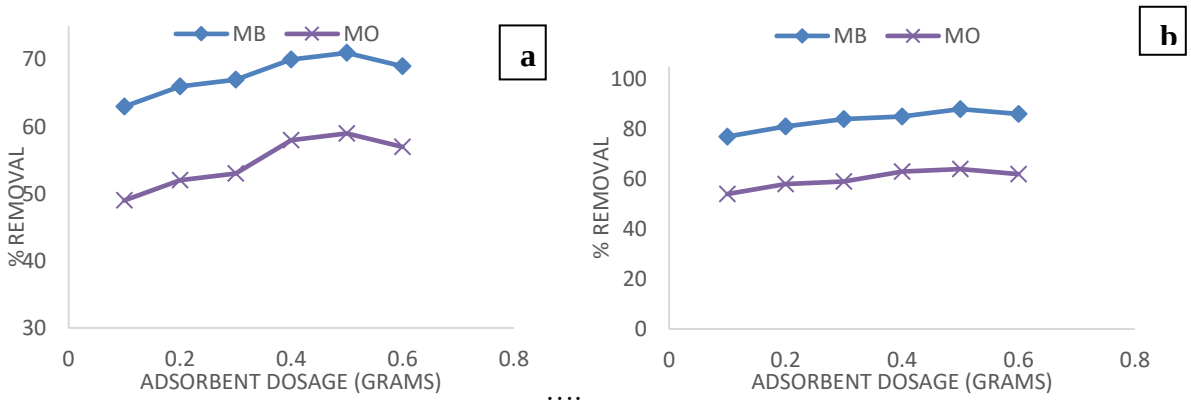

Figure 7: Effect of Adsorbent Dosage on MB and MO adsorption onto (a) Cellulose and (b) Cel/TiO_2 NCs

Effect of pH

The effect of pH on the adsorption of MB and MO onto Cellulose and Cel/TiO_2 NCs from aqueous solution was studied in the pH range of 2 – 12 keeping other parameters constant. The results are shown in Figure 8, it was observed that the optimum pH for the adsorption of MB and RhB is 8 while 4 and 6 for MO and CR respectively.

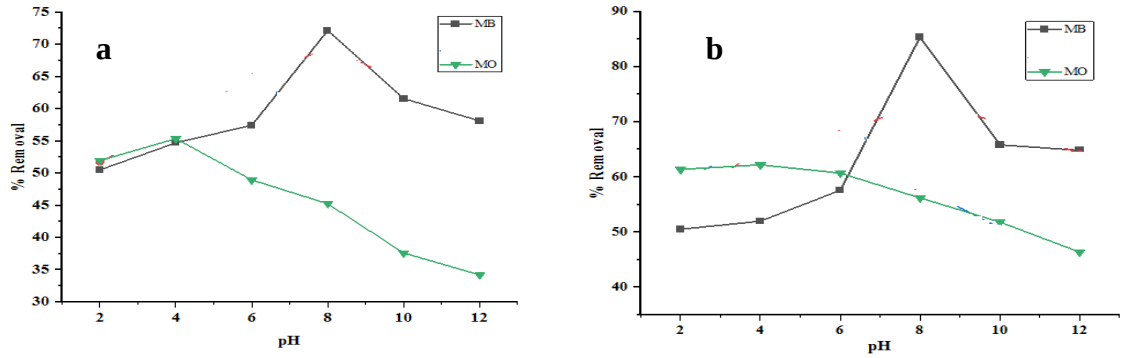

Figure 8: Effect of pH on MB and MO adsorption onto (a) Cellulose and (b) Cel/TiO_2 NCs

Kinetics

The kinetics studies of the adsorption system describe the rate of adsorbate uptake on adsorbent and also helps to determine the equilibrium time for the adsorption. The pseudo-first order and pseudo-second order models were used to predict the adsorption behavior of MB and MO onto Cellulose and Cel/TiO_2 NCs the results are shown in Figures 9 and 10 above and summarized in Table 1. The results showed that the correlation coefficient (R^2) for pseudo-second order model were higher than that of pseudo-first order model for all the adsorption processes. This showed that the pseudo-second order model was therefore, the best fitted kinetics model for the adsorption of both the cationic and anionic dyes. The Adsorption isotherm is used to study how the adsorbate molecules are distributed between the liquid phase and adsorbent (Birniwa *et al.*, 2022).

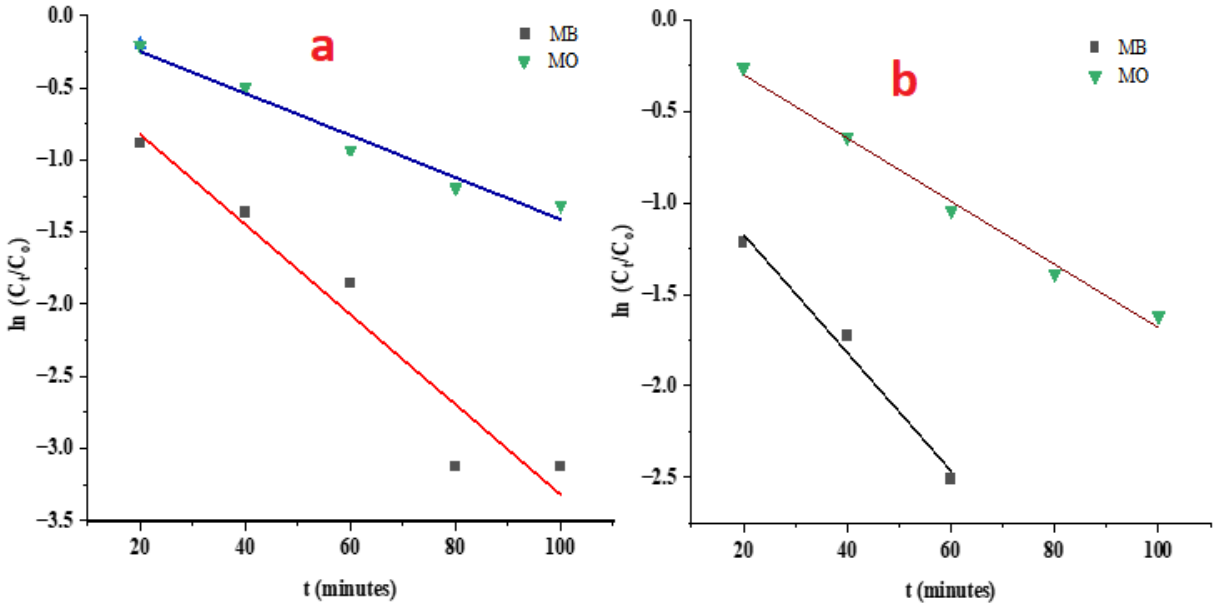

Figure 9: Pseudo-first order plot for adsorption of MB, RhB, CR and MO onto (a) Cellulose and (b) Cel/TiO_2 NCs

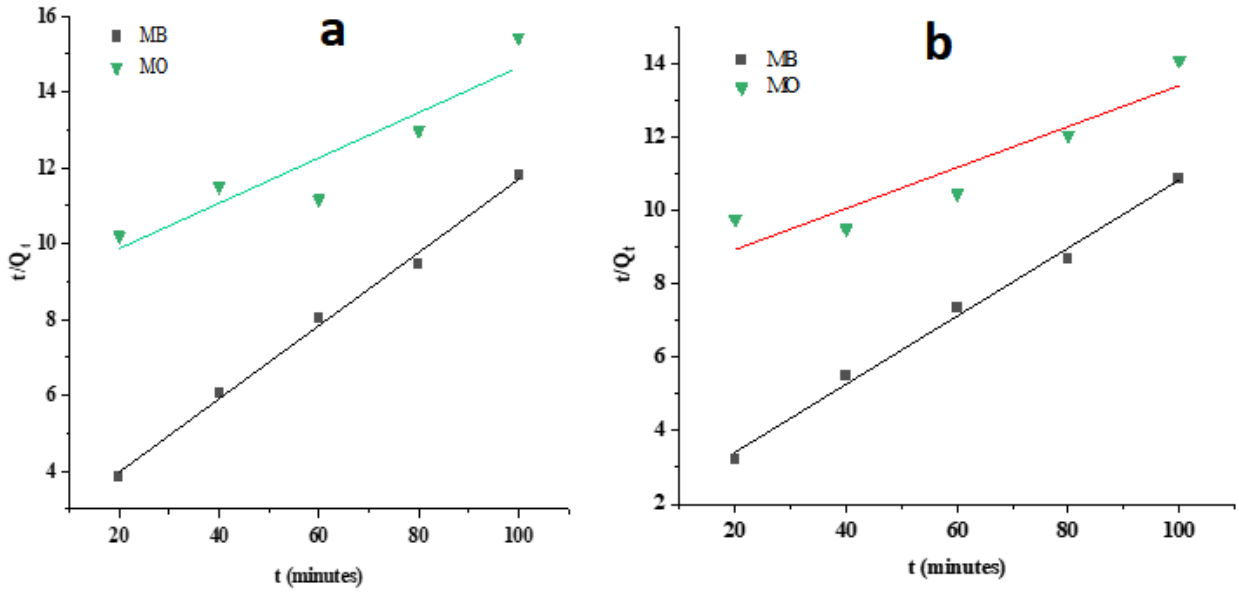

Figure 10: Pseudo-second order plot for adsorption of MB and MO onto (a) Cellulose and (b) Cel/TiO_2 NCs

Table 1: Kinetics Parameters for the Pseudo-first-order and Pseudo-second-order for the Adsorption of MB, and MO onto Cellulose Extract and Cel/TiO_2 NCs

Adsorbent	Adsorbate	Pseudo-first order		Pseudo-second order		
		R^2	k_1	R^2	Q_e(exp)	k_2
Cellulose	MB	0.91087	0.03124	0.9949	10.366	0.00222
	MO	0.9564	0.01458	0.81074	16.748	0.000411
Cel/TiO_2 NCs	MB	0.96917	0.0323	0.99103	10.78	0.005513
	MO	0.98842	0.01728	0.81553	17.88	0.000399

Thermodynamic Results

The thermodynamic behaviour for MB and MO adsorption onto Cellulose and Cel/TiO_2 NCs was studied. The Gibb's free energy, Enthalpy changes and Entropy were obtained, the results were tabulated and shown in Table 2 and Figure 11. The negative value of ΔG for MB and MO adsorption onto Cellulose extract and Cel/TiO_2 NCs at six experimental temperature indicates that the adsorption process is spontaneous endothermic and feasible. The positive values of ΔH suggested an endothermic nature of the adsorption process. Moreover, the positive ΔS values indicate the spontaneity and affinity of the dyes toward Cellulose and Cel/TiO_2 NCs, and also reflect the increased randomness at the solid/solution interface (Ahmad & Ansari, 2021).

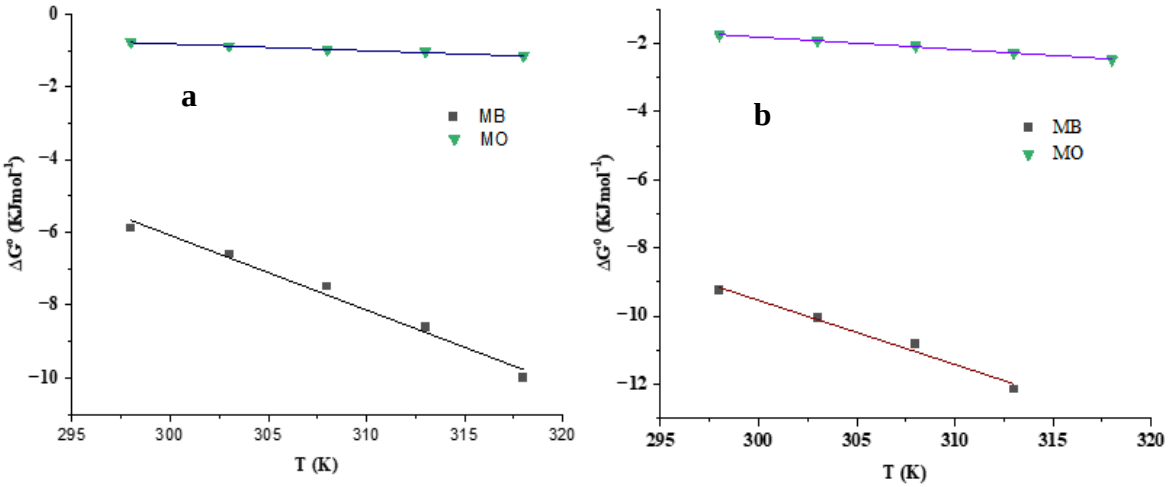

Figure 11: Thermodynamics plot for adsorption of MB and MO onto (a) Cellulose and (b) Cel/TiO_2 NCs

Table 2: Thermodynamics Parameters for the Adsorption of MB and MO onto Cellulose Extract and Cel/TiO_2 NCs

Adsorbent	Adsorbate	ΔH (kJ/mol)	ΔS(J/K)	ΔG(kJ/mol)
Cellulose	MB	55.22	204.35	-5.886
	MO	4.76	18.58	-0.771
Cel/TiO_2 NCs	MB	105.95	383.12	-9.264
	MO	8.94	35.84	-1.749

Isotherm Results

The results of isotherm studies for the MB and MO onto Cellulose and Cel/TiO_2 NCs were presented in Figures 12 – 19 and summarized in Table 3, Langmuir and Freundlich isotherm model were applied to analyze the adsorption experiment data. It was seen from Table 3 that R^2 values for Langmuir isotherm were higher than that of the Freundlich isotherm model, this indicates that the Langmuir isotherm model a better fit than the Freundlich model and the adsorption mechanism was chemisorption. These results suggested that monolayer adsorption of MB and MO onto the cellulose and Cel/TiO_2 NCs occurred. However, the dimensionless separation factor R_L values are in the range of 0 – 1 indicating that the adsorption process is favourable.

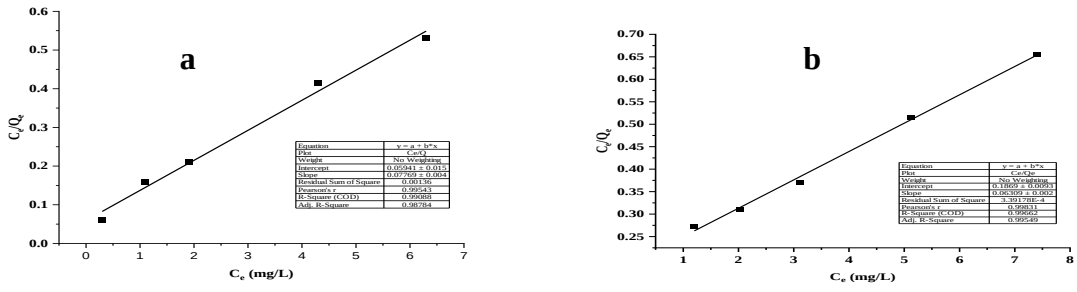

Figure 12: Langmuir Isotherm for adsorption of (a) MB and (b) MO onto Cellulose

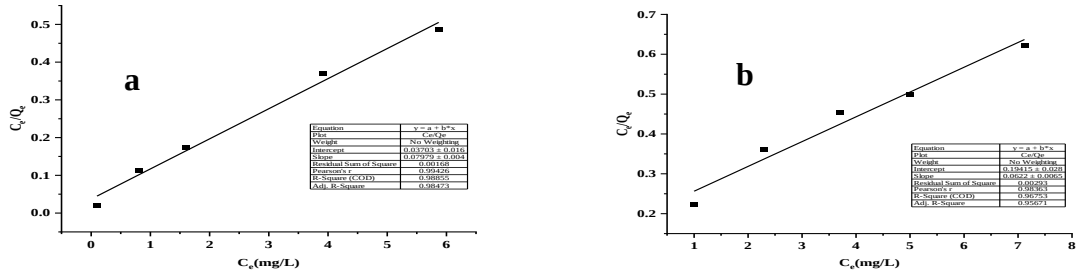

Figure 13: Langmuir Isotherm for adsorption of (a) MB and (b) MO onto Cel/TiO_2 NCs

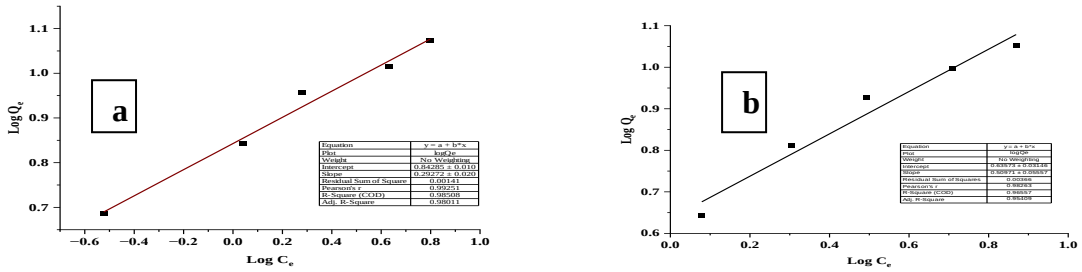

Figure 14: Freundlich isotherm plot for adsorption of (a) MB and (b) MO onto Cellulose

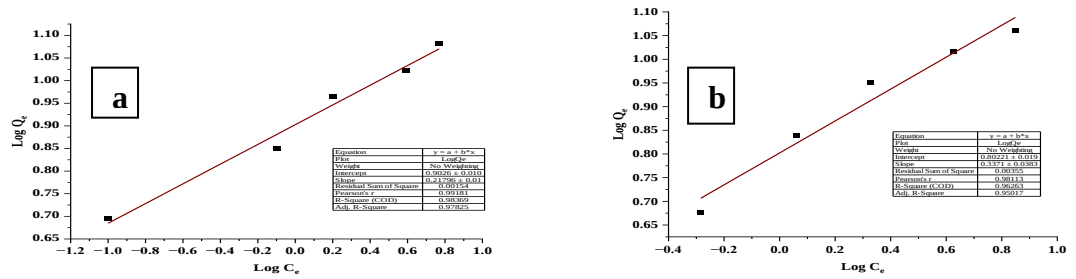

Figure 15: Freundlich isotherm plot for adsorption of (a) MB and (b) MO onto Cel/TiO_2 NCs

Table 3: Adsorption Isotherm Parameters for the Adsorption of MB and MO onto Cellulose Extract and Cel/TiO_2 NCs

Adsorbent	Adsorbate	Langmuir				Freundlich		
		Q_m (mg/g)	K_L (L/mg)	R^2	R_L	N	K_F ((mg/g)(L/mg))$^{1/n}$	R^2
Cellulose	MB	12.872	1.308	0.988	0.025	3.416	2.323	0.980
	MO	15.850	0.338	0.995	0.090	1.962	1.888	0.954
Cel/TiO_2 NCs	MB	12.533	2.155	0.985	0.015	4.588	2.466	0.978
	MO	16.077	0.320	0.957	0.094	1.875	1.845	0.987

Reusability study

The reusability of an adsorbent is an important parameter to analyze its potentiality for an industrial application and to solve the problem of excessive adsorbent disposal. Reusability studies were carried out on MB adsorbed cellulose and Cel/TiO_2 NCs adsorbents, the results in Figure 20 showed that the removal efficiency of cellulose decreased to 63.11 % while that of Cel/TiO_2 decreased to 67.81% after five adsorption-desorption cycles. This shows that the adsorbents possess excellent ability to be reused for dye removal.

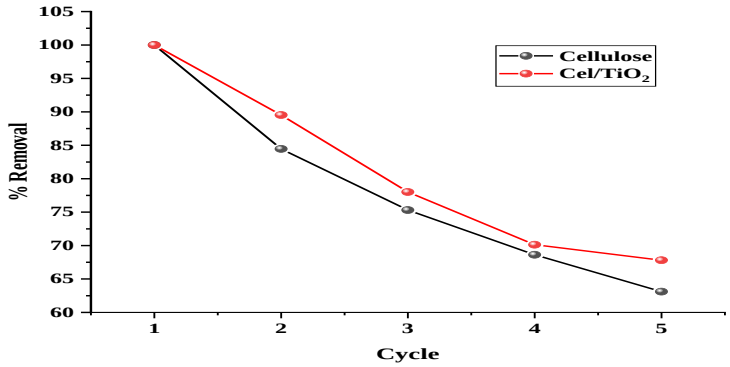

Figure 16: Reusability study on Cellulose and Cel/TiO_2 NCs

CONCLUSION

In this study, cellulose was successfully extracted from millet husk using the Alkaline-Hydrogen peroxide method and Cel/TiO_2 NCs were synthesized via sol – gel method. The isolated cellulose material was used to improve the adsorption efficiency of TiO_2. The adsorbents were characterized using FTIR, SEM and XRD techniques. The optimal conditions for adsorption were found to be 0.5g/100ml at an initial dye concentration of 18mg/L, 25^{o}C, a pH of 8 for MB and 25 minutes, a pH of 6 and 4 for MO. The crystal size of Cel/TiO_2 NCs was calculated to be 27.6nm using Scherrer equation. The adsorption data showed that a pseudo-second-order model of adsorption kinetics and the Langmuir model for adsorption isotherm gave the best fit. Thermodynamic analyses indicated that the adsorption process was chemisorptive, spontaneous, feasible and endothermic.

REFERENCES

Ahmad, R., & Ansari, K. (2021). Comparative study for adsorption of congo red and methylene blue dye on chitosan modified hybrid nanocomposite. *Process Biochemistry*, *108*, 90-102.

Birniwa, A. H., Mahmud, H. N. M. E., Abdullahi, S. S. a., Habibu, S., Jagaba, A. H., Ibrahim, M. N. M., Ahmad, A., Alshammari, M. B., Parveen, T., & Umar, K. (2022). Adsorption behavior of methylene blue cationic dye in aqueous solution using polypyrrole-polyethylenimine nano-adsorbent. *Polymers*, *14*(16), 3362.

Dutta, S., Adhikary, S., Bhattacharya, S., Roy, D., Chatterjee, S., Chakraborty, A., Banerjee, D., Ganguly, A., Nanda, S., & Rajak, P. (2024). Contamination of textile dyes in aquatic environment: Adverse impacts on aquatic ecosystem and human health, and its management using bioremediation. *Journal of Environmental Management*, *353*, 120103.

Ghosh, S., & Das, A. (2015). Modified titanium oxide (TiO2) nanocomposites and its array of applications: a review. *Toxicological & Environmental Chemistry*, *97*(5), 491-514.

Giwa, A., Yusuf, A., Balogun, H. A., Sambudi, N. S., Bilad, M. R., Adeyemi, I., Chakraborty, S., & Curcio, S. (2021). Recent advances in advanced oxidation processes for removal of contaminants from water: A comprehensive review. *Process Safety and Environmental Protection*, *146*, 220-256.

Guerra, F. D., Attia, M. F., Whitehead, D. C., & Alexis, F. (2018). Nanotechnology for environmental remediation: materials and applications. *Molecules*, *23*(7), 1760.

Habibu, S., Ladan, M., Safana, A. A., Dandalma, Z. A., Saleh, I., & Abdullahi, S. R. (2023). Optimization of Methylene Blue Adsorption onto Activated Carbon derived from Pineapple Peel Waste using Response Surface Methodology. *UMYU Scientifica*, *2*(4), 45-55.

Katheresan, V., Kansedo, J., & Lau, S. Y. (2018). Efficiency of various recent wastewater dye removal methods: A review. *Journal of environmental chemical engineering*, *6*(4), 4676-4697.

Khalil, H. A., Bhat, A., & Yusra, A. I. (2012). Green composites from sustainable cellulose nanofibrils: A review. *Carbohydrate polymers*, *87*(2), 963-979.

Khan, S., Naushad, M., Al-Gheethi, A., & Iqbal, J. (2021). Engineered nanoparticles for removal of pollutants from wastewater: Current status and future prospects of nanotechnology for remediation strategies. *Journal of environmental chemical engineering*, *9*(5), 106160.

Khin, M. M., Nair, A. S., Babu, V. J., Murugan, R., & Ramakrishna, S. (2012). A review on nanomaterials for environmental remediation. *Energy & Environmental Science*, *5*(8), 8075-8109.

Ladan, M., Basirun, W. J., & Kazi, S. N. (2021). Polyaniline/graphene oxide/Zn-doped TiO2 nanocomposite coatings for the corrosion protection of carbon steel. *Journal of Adhesion Science and Technology*, *35*(22), 2483-2505.

Li, Y., Yin, X., Huang, X., Tian, J., Wu, W., & Liu, X. (2019). The novel and facile preparation of 2DMoS2@ C composites for dye adsorption application. *Applied Surface Science*, *495*, 143626.

Li, Z., Qiu, F., Yue, X., Tian, Q., Yang, D., & Zhang, T. (2021). Eco-friendly self-crosslinking cellulose membrane with high mechanical properties from renewable resources for oil/water emulsion separation. *Journal of environmental chemical engineering*, *9*(5), 105857.

Ma, Y., Wang, X., Jia, Y., Chen, X., Han, H., & Li, C. (2014). Titanium dioxide-based nanomaterials for photocatalytic fuel generations. *Chemical reviews*, *114*(19), 9987-10043.

Mahlambi, M. M., Ngila, C. J., & Mamba, B. B. (2015). Recent developments in environmental photocatalytic degradation of organic pollutants: the case of titanium dioxide nanoparticles—a review. *Journal of Nanomaterials*, *2015*(1), 790173.

Mehra, S., Singh, M., & Chadha, P. (2021). Adverse impact of textile dyes on the aquatic environment as well as on human beings. *Toxicol. Int*, *28*(2), 165.

Rashid, M. M., Shen, X., Islam, S. R., Al Mizan, R., & Hong, Y. J. J. o. W. P. E. (2022). Sono-synthesis of cellulose-TiO_2 nanocomposite adsorbent for fast cleaning of anionic dyes containing wastewater. *47*, 102799.

Shaghaleh, H., Xu, X., & Wang, S. (2018). Current progress in production of biopolymeric materials based on cellulose, cellulose nanofibers, and cellulose derivatives. *RSC advances*, *8*(2), 825-842.

Sheltami, R. M., Abdullah, I., Ahmad, I., Dufresne, A., & Kargarzadeh, H. (2012). Extraction of cellulose nanocrystals from mengkuang leaves (Pandanus tectorius). *Carbohydrate polymers*, *88*(2), 772-779.

Srivastava, R., & Sofi, I. R. (2020). Impact of synthetic dyes on human health and environment. In *Impact of textile dyes on public health and the environment* (pp. 146-161). IGI Global.

Tang, C., Wang, B., Wang, H. F., & Zhang, Q. (2017). Defect Engineering toward Atomic Co–Nx–C in Hierarchical Graphene for Rechargeable Flexible Solid Zn-Air Batteries [Article]. *Advanced Materials*, *29*(37), Article 1703185. https://doi.org/10.1002/adma.201703185

Yang, L., Chen, C., Hu, Y., Wei, F., Cui, J., Zhao, Y., Xu, X., Chen, X., & Sun, D. (2020). Three – dimensional bacterial cellulose/polydopamine/TiO_2 nanocomposite membrane with enhanced adsorption and photocatalytic degradation for dyes under ultraviolet-visible irradiation. *Journal of colloid and interface science*, *562*, 21-28.